A new class of electrorheological material: synthesis and electrorheological performance of rare earth complexes of phosphate cellulose

ZHI-WEI PAN, YAN-LI SHANG, JUN-RAN LI*, SONG GAO
State Key Laboratory of Rare Earth Materials Chemistry and Applications, College of Chemistry and Molecular Engineering, Peking University, Beijing 100871, P. R. China
E-mail: lijunran@pku.edu.cn

YAN-LI SHANG
Department of Chemistry, Hebei Normal University, Shijiazhuang 050091, China

RUI-LI HUANG
Frederick, Maryland 21702, USA

JUAN WANG, SHAO-HUA ZHANG
School of Vehicle and Transmission Engineering, Beijing Institute of Technology, Beijing 100081, China

YUAN-JING ZHANG
Department of Chemistry, Shijiazhuang college, Shijiazhuang 050035, China

Published online: 12 January 2006

A new class of electrorheological (ER) material, rare earth (RE = Ce, Gd, Er and Y) complexes of phosphate cellulose, has been synthesized using microcrystalline cellulose, phosphoric acid, urea and $RE(NO_3)_3$ solutions as starting materials. The ER properties of suspensions of microcrystalline cellulose, phosphate cellulose [cellulose-P-ONH_4] and the [cellulose(-P-O)$_3$RE] complex particle materials in silicon oil have been investigated under DC electric field. The formation of rare earth complexes helps to decrease the shear stress and viscosity at zero electric field, and to enhance the ER effect of the materials. The shear stress (τ_E) of the ER fluid (20% weight fraction) of a typical yttrium complex [cellulose(-P-O)$_3$Y], the yttrium content of which is 0.04 mol/100 g, is 2.3 kPa at 4.2 kV/mm and 300 s^{-1} with a τ_r value ($\tau_r = \tau_E/\tau_0$, where τ_0 is the shear stress at no electric field and 300 s^{-1}) of 34.3, which is 18 times higher than that of pure microcrystalline cellulose suspensions. The improvement of dielectric loss tangent of the material, due solely to the formation of rare earth complexes, resulted in an enhancement in the ER effect of the material. In addition, the cellulose(-P-O)$_3$RE materials possess better thermal stability, and their suspensions are more stable in the anti-sedimentation than that of the cellulose-P-ONH_4 material.

1. Introduction

An electrorheological (ER) fluid is a suspension consisting of dielectric particles and an insulating liquid. The rheological properties (viscosity, yield stress, shear modulus, etc.) of an ER suspension could change reversibly, by several orders of magnitude, under an external electric field with a several kilovolts per millimeter strength. Since its mechanical properties can be easily controlled within a wide range, the ER fluid could be used as an electric and mechanical medium in various industrial applications. For example, it could be used in the automotive industry for clutch, brake and damping systems [1]. It could also be used in other areas, such as polishing, ink jet printers, human muscle stimulators, mechanical sensors, and so on [2–4]. Furthermore, ER fluids could be used to in building optical or microwave devices and periodic dielectric

*Author to whom all correspondence should be addressed.
0022-2461
DOI: 10.1007/s10853-005-2329-5

superstructure crystals because of their unique structural characteristics exhibited under an electric field [5–10]. Most ER fluids are made of solid particle materials dispersed into an insulating non-polar liquid.

Before 1985, all ER fluids contained small amounts of water. Such ER fluids have many shortcomings, such as narrow working temperature range, high current density, as well as device erosion caused by water [1]. Anhydrous ER fluids are believed to be more promising for industrial applications. They have thus received greater attention later on, and various types of water-free ER fluids have been developed since [11, 12]. The solid, particulate material in the ER fluid can be made of inorganic, organic, or polymeric materials. The inorganic materials include inorganic oxides such as silica, titanium dioxide and piezoelectric ceramics. They tend to adsorb water easily, which is a drawback for this type of inorganic materials. Examples of non-oxide inorganic materials include aluminosilicates and zeolite. Although non-oxide inorganic materials do not contain water and may have strong ER effects, the ER fluids made of inorganic materials generally have a much denser their dispersed phase than the dispersing medium, which would usually lead to unstable suspensions. In addition, inorganic particles are hard in nature and would be abrasive to the ER device where the ER fluid is applied. Consequently, organic and polymeric materials, such as acene-quinone radical polymers, polyacrylonitrile, polymethyl acrylic acid, starch and dextran, are believed to be better than inorganic materials. ER fluids containing these materials have been investigated intensively as a result [1]. However, the ER effect of organic and polymeric ER fluids is not as strong as those containing non-oxide inorganic materials. It is clear that the ER performance of a material is closely related to the conductivity and polarizability of the material, thus the ER performance of the organic or polymeric materials can be improved by adjusting their molecular structures.

The ER effect of anhydrous cellulose is weak. The ER activity of dried phosphate cellulose particles obtained by esterification of cellulose with an orthophosphoric acid-urea mixture is much stronger than that of anhydrous cellulose [13–17]. In order to find an ideal ER material that not only possesses better ER performance, but also is economical and facile; and to obtain a better understanding on the mechanism of the ER effect, we have synthesized a new type of ER material, the rare earth (RE = Ce, Gd, Er and Y) complexes of phosphate cellulose. Here we report the investigation of the ER properties of these compounds and novel results acquired therein.

2. Experimental

2.1. Synthesis of the rare earth complex particles

All reagents, except for microcrystalline cellulose, were provided by Beijing Chemistry Reagent Co. (China) and used without further purification. Phosphate cellulose particles were synthesized by esterification of cellulose with an orthophosphoric acid-urea mixture (phosphorylation of cellulose) at room temperature, using the method reported by Kim S.G. *et al*. [16]. At first, a mixture containing 109 g urea, 64.8 cm^3 phosphoric acid (orthophosphoric acid, concentration 15 M) and 310 cm^3 distilled water was stirred at room temperature for 1 h, to form a clear solution. Cellulose particles (31.6 g), with an average size of ca.100 nm (ARBOCEL, Type P290, JRS, Holzmühle 1 D-43494 Rosenberg, Germany), were then added to the solution and stirred for 42 h to allow the phosphoric ester reaction of cellulose.

After the reaction, the phosphate cellulose particles were washed three times with an aqueous solution of ethanol (H_2O: CH_3CH_2OH = 1:1 volume ratio), and then washed three times with anhydrous ethanol to remove any unreacted urea and phosphoric acid. After drying at 60 °C for 4 h, the phosphate cellulose particles were grounded and dried at 150°C for 2 h. The grounded products were dried finally at room temperature in a vacuum oven until no more weight change was observed, in order to remove any residual water. The phosphate cellulose particle material (Sample 2) was thus obtained.

After washing and drying at 60°C for 30 min, the phosphate cellulose particles were dispersed in an aqueous solution of $RE(NO_3)_3$. The reaction mixture was stirred first at 50–60°C for 1 h and then continuously at room temperature for another 22 h. The particle materials containing RE were dried by following a similar procedure as described above.

2.2. Preparation of the ER fluids and electrorheological experiment

The electrorheological experiments were carried out using a German Rotary Viscometer (Type HAAKE CV20). The apparatus can function at the desired temperature and electrode clearance to measure the anti-shear stress and apparent viscosity of a fluid at various shear states; and it has various operating modes such as rate control, stress control and oscillation. The measurements were carried through in a ZA15 sensor system, which consists of a pair of coaxial cylinders with a 0.545 mm gap in between. The system is connected to a power supply, the voltage of which can be controlled and adjusted from 0 to 5 kV/mm. The suspensions are placed in the gap, with the inner cylinder kept stationary and the outer cylinder rotating at preconcerted rates while the apparatus is operating. The measured ranges are 0–3000 Pa for shear stress and 0–300 s^{-1} for shear rate ($\dot{\gamma}$). In this paper, the sample shear stresses and viscosities have been determined under different electric field strengths (E, dc field) at a given temperature (20°C).

The microcrystalline cellulose, phosphate cellulose or the complex particle materials were mixed quickly, after water removal, with dimethyl silicone oil (density $\rho = 0.98$ g·cm^{-3} and viscosity $\eta = 98$ mPa·s at 25°C) under stirring and ultrasonically dispersing for five minutes, to yield the ER fluid (20% weight fraction) samples. The

TABLE I Composition of polymer materials

Sample no	Composition	N Content (wt.%(mol/100 g))	P Content (wt.% (mol/100 g))	RE Content (wt.% (mol/100 g))	$\Delta n_N/n_{RE}$[a]
1	Cellulose				
2	Cellulose-P-ONH_4	4.19 (0.299)	7.71 (0.249)		
3	Cellulose(-P-O)$_3$Ce	2.31 (0.165)	7.62 (0.246)	5.99 (0.043)	3.1
4	Cellulose(-P-O)$_3$Gd	2.47 (0.176)	7.69 (0.248)	5.70 (0.036)	3.4
5	Cellulose(-P-O)$_3$Er	2.41 (0.172)	7.54 (0.243)	5.94 (0.036)	3.5
6	Cellulose(-P-O)$_3$Y	2.46 (0.176)	7.72 (0.249)	3.26 (0.037)	3. 3

[a] Δn_N represents the difference in nitrogen content (mol/100 g) between cellulose-P-ONH_4 and cellulose(-P-O)$_3$RE materials; n_{RE} represents RE content (mol/100 g) in cellulose(-P-O)$_3$RE material.

suspensions were then put in the gap between the cylinders as soon as possible for electrorheological experiments.

2.3. Characterization of the materials

The N and P contents in the materials were determined on a German Elementar Vario EL instrument and an IRIS/AP plasma spectrometer, respectively; the RE contents of the materials were confirmed by titration using an EDTA solution and 3,3′-Bis[N,N-di(carboxymethyl)aminomethyl]-o-cresolsulphon naphthalein as an indicator. IR spectra were measured using KBr pellets with a Nicolet Magna-IR 750 spectrometer at 295 K. Thermal analyses were performed on a Du Pont 1090B thermal analyzer. The average grain sizes of the particle materials were measured on a S-3000N Scanning Electron Microscope manufactured by Hitachi Science Systems, Ltd. in Japan. The surface areas of the particle materials were measured on an ASAP 2010 Accelerated Surface Area & Porosimetry apparatus made by the US Micromeritics Company.

3. Result and discussion

3.1. Composition of materials

The elemental analysis results (see Table I) show that there are N and P elements with a molar ratio of 1:1 in sample 2. This fact proves that ammonium ions exist in the phosphate cellulose, namely ammonium salt of the phosphate cellulose has been obtained by esterification of cellulose, indicating that the H^+ ions from the P-OH groups of the phosphate cellulose are replaced by ammonium ions. After the reaction between the salt and $RE(NO_3)_3$, the ammonium ions are substituted by the rare earth ions (RE^{3+}) with an ammonium ion to RE^{3+} molar ratio of 3:1, consistent with charge equilibrium, to form the rare earth complex of phosphate cellulose. Therefore, the conversion process from cellulose to the rare earth complex of phosphate cellulose can be roughly illustrated as the following:

$$\text{Cellulose} \xrightarrow{H_3PO_4,\,\text{urea}} \text{Cellulose-P-}ONH_4$$
$$\xrightarrow{RE(NO_3)_3} \text{Cellulose(-P-O)}_3\text{RE}$$

The material compositions are listed in Table I.

The IR spectra (see Fig. 1, the IR spectra of samples 3–6 are very similar, so, that of sample 3 was selected as a representation.) of the materials provide further evidence for the transformation process described above [18, 19]. Comparing sample 2 to sample 1, the new strong peaks appeared at 3289 cm^{-1} and 1449 cm^{-1} indicate the presence of ammonium ions in the polymeric molecule of sample 2; the new strong peak appeared at 1231 cm^{-1} is characteristic of a -P=O group. In the IR spectra of samples 3–6, we can see that the characteristic absorption of an O-RE bond appeared at 214c m^{-1}; comparing with sample 2, the characteristic absorptions of ammonium ions

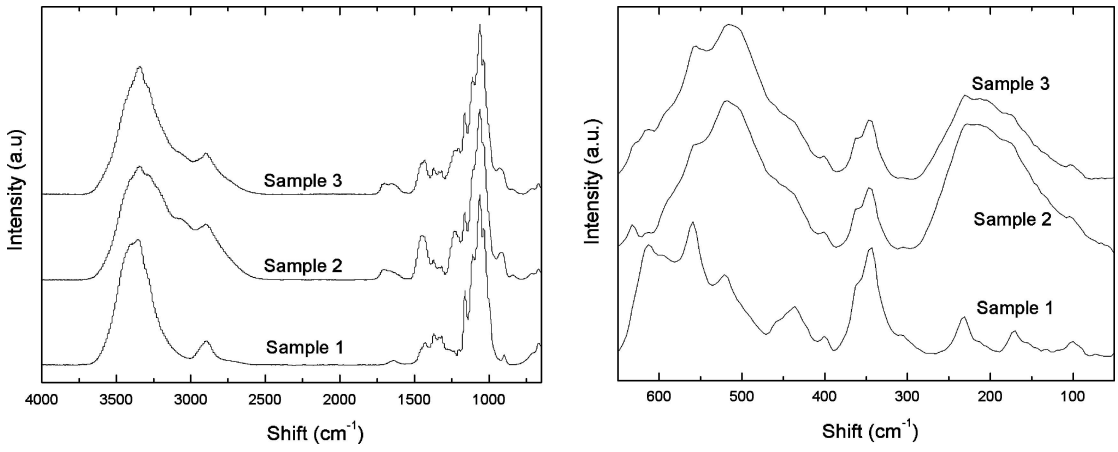

Figure 1 IR spectra of samples.

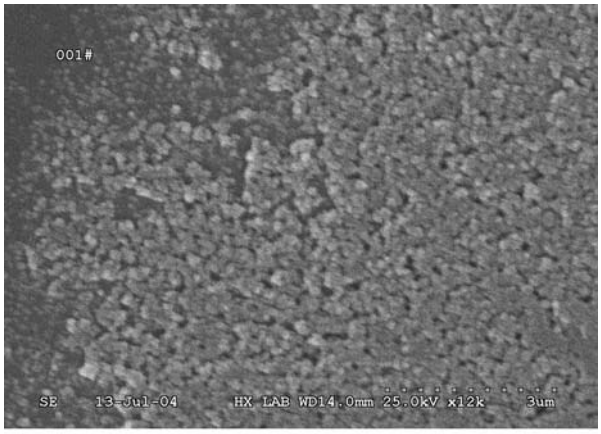

(a)

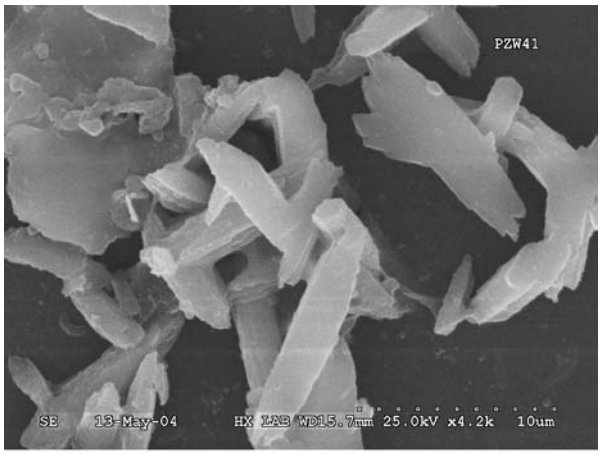

(b)

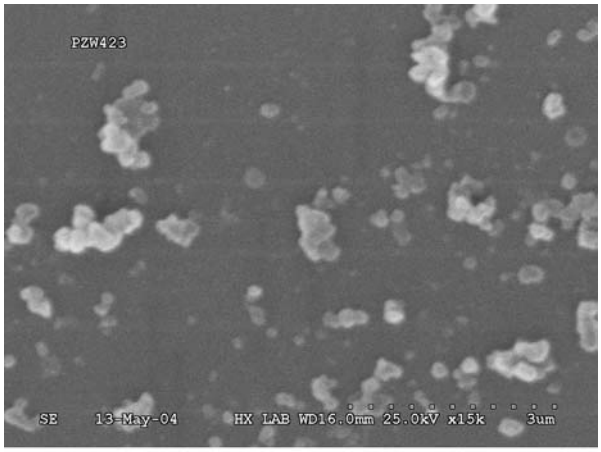

(c)

Figure 2 SEM photographs of cellulose (a), cellulose-P-ONH_4 (b) and cellulose-$(P\text{-}O)_3Ce$ (c) particles.

are weakened to shoulder peaks, and two new peaks appeared at 1205 and 1229 cm^{-1}, which could be the result of a split in the -P=O bond vibration peak (1231 cm^{-1}) after coordination to a rare earth ion. These results have confirmed that sample 3–6 are the rare earth complexes, which are the products of partial ammonium ion substitution in the polymeric molecule of sample 2 by rare earth ions.

Fig. 2 illustrates the SEM photographs of cellulose (a), cellulose-P-ONH_4 (b) and cellulose-$(P\text{-}O)_3Ce$ (c) particles (SEM photographs of other cellulose-$(P\text{-}O)_3RE$ particles are similar to that of the cellulose-$(P\text{-}O)_3Ce$ particles). The cellulose particles are sphere-like with an average diameter of ca. 100 nm, the cellulose-P-ONH_4 material are composed of rod-like (ca. $0.3 \times 1\ \mu m$) and irregular particles, and the cellulose-$(P\text{-}O)_3Ce$ particles are amorphous with an average diameter of ca. 100–200 nm. The changes in the shape and size of the particles may be ascribed to a translation reaction from the cellulose to the cellulose-P-ONH_4 and the cellulose-$(P\text{-}O)_3Ce$.

3.2. The ER effect and dielectric property of materials

In order to obtain a clear comparison of the ER effect of the materials, three types of viscosity were employed: the apparent viscosity of the suspension with and without applied electric field (η_E and η_0, respectively), and relative viscosity (η_r), which is defined in our work as the ratio of apparent viscosity to zero-field viscosity ($\eta_r = \eta_E/\eta_0$). The η values of the corresponding ER fluids (20% weight fraction) for the samples at 20°C, $E = 4.2$ kV and $\dot{\gamma} = 300\ S^{-1}$, are listed in Table II.

The η_r values in Table II indicate that the ER effect ($\eta_r = 1.85$) of dried microcrystalline cellulose (Sample 1) is very weak. The cellulose-P-ONH_4 and cellulose-$(P\text{-}O)_3RE$ (RE=Ce, Gd, Er and Y) materials all exhibit obvious ER behavior; the η_r values of the cellulose-$(P\text{-}O)_3RE$ suspensions are larger than that of the cellulose-P-ONH_4 suspension ($\eta_r = 3.88$), indicating that the cellulose-$(P\text{-}O)_3RE$ materials have better ER activity than the cellulose-P-ONH_4 material. The η_r value (34.3) of the cellulose-$(P\text{-}O)_3Y$ suspension is the largest, which is 18 times larger than that of sample 1; and the η_r values of the cellulose-$(P\text{-}O)_3RE$ (RE = Ce, Gd and Er) suspensions are comparable. Therefore, the ER performance of the cellulose-$(P\text{-}O)_3Y$ material is the best among these materials, and the other cellulose-$(P\text{-}O)_3RE$ materials have similar ER activity. From the η_0 values of the suspensions in Table II, we can see that the η_0 values of the cellulose-$(P\text{-}O)_3RE$ suspensions are all smaller than that of the cellulose-P-ONH_4 suspension, which can be ascribed to lower density for the cellulose-$(P\text{-}O)_3RE$ material than for the cellulose-P-ONH_4 material, with forming the complex between RE^{3+} ions and cellulose-$P\text{-}O^-$ ions (see Section 3.4); namely, replacing ammonium ions with RE ions would lower the viscosity of the suspensions, which may be an important indication that the ER performance of the materials could be improved with the presence of the rare earth complexes. The cellulose-$(P\text{-}O)_3Er$ suspension has a larger η_r value (24.3) than the cellulose-P-ONH_4 suspension (3.88), even though its η_E value (4057 mPa·s) is smaller than that of the cellulose-P-ONH_4 suspension (4786 mPa·s).

Fig. 3 illustrates the electric field strength dependence of the shear stress of the ER suspensions of samples 1–6

TABLE II Viscosity and dielectric property of the suspensions

Sample no	Composition	η_0 (mPa·s)	η_E (mPa·s)	η_r	ε	$tg\delta$
1	Cellulose	176.7	327.5	1.85	1.36	0.015
2	Cellulose-P-ONH_4	1235	4786	3.88	1.67	0.029
3	Cellulose(-P-O)$_3$Ce	319.8	8160	25.5	1.46	0.063
4	Cellulose(-P-O)$_3$Gd	409.5	9562	23.4	1.52	0.038
5	Cellulose(-P-O)$_3$Er	166.9	4057	24.3	1.90	0.067
6	Cellulose(-P-O)$_3$Y	221.0	7577	34.3	2.25	0.092

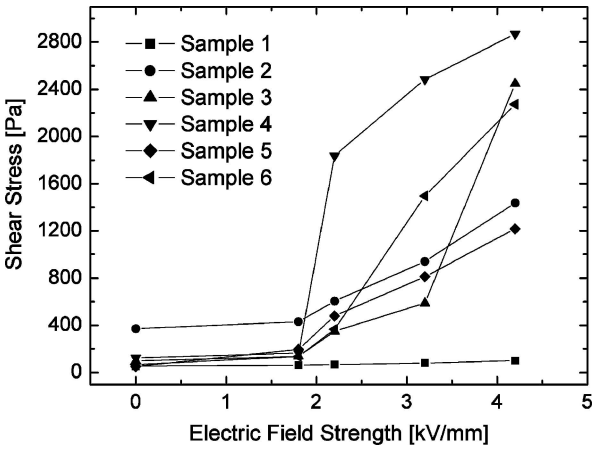

Figure 3 Electric field strength dependence of shear stress of the suspensions of samples 1–6.

at 300 S^{-1}. The shear stress of the suspension of sample 1 is very low with little change at increasing electric field strength. For sample 2, the shear stress of the suspension increases with electric field strength, showing the ER activity. The ER behavior of samples 3–6 [cellulose(-P-O)$_3$RE] is clearly different from that of sample 2 (cellulose-P-ONH_4), the shear stresses of their suspensions are much lower than that of sample 2 at $E \leq 1.8$ kV/mm. However, four cellulose(-P-O)$_3$RE materials display different ER behaviors at $E > 1.8$ kV/mm. For the cellulose(-P-O)$_3$Gd material (sample 4), the shear stress of the suspension increases markedly at $E > 1.8$ kV/mm, reaching 2.9 kPa, which is the highest among the suspensions of all materials, at $E = 4.2$ kV/mm; whereas at zero electric field, the shear stress of this suspension is higher (122.9 Pa) than that of the suspensions of cellulose(-P-O)$_3$RE (RE = Y, Ce and Er); thus, its ER effect ($\eta_r = 23.4$) is weaker than those of samples 3, 5 and 6 (η_r = 25.5, 24.3 and 34.3, respectively). The shear stresses of the cellulose(-P-O)$_3$Y and cellulose(-P-O)$_3$Ce suspensions are higher than that of sample 2 at $E > 2.5$ kV/mm and $E > 3.5$ kV/mm, respectively; and they reach 2.3 kPa and 2.4 kPa, respectively, at E=4.2 kPa. In contrast with sample 2, the shear stress of the cellulose(-P-O)$_3$Er suspension (sample 5) is always lower, the shear stress without an electric field is much lower (50.1 Pa), and it is only slightly lower than that of sample 2 at $E \geq 2.2$ kV/mm. Therefore, the suspension of sample 5 has a larger η_r value, and the ER effect of the cellulose(-P-O)$_3$Er material should be better than that of the cellulose-P-ONH_4 material. In conclusion, the ER performance of microstructure cellulose can be improved by joining the -P-ONH_4 polar groups in the polymer chain; joining the -P-ORE (RE = Ce, Gd, Er and Y) polar groups, that is to say, the presence of the rare earth complex, can enhance the ER activity of the material more effectively.

The difference in the ER properties of these materials can be explained by their dielectric properties. Because of the difficulties involved in directly measuring the dielectric properties, the suspensions (20%, weight fraction) of the materials were used to carry out the dielectric investigation. The capacitance C and dielectric loss tangent (tan δ) at room temperature were obtained on a HP4274A Multi-frequency LCR Meter. The dielectric constant (ε) of the suspensions were derived from the measured C according to the conventional relation, $\varepsilon = C \cdot d/(\varepsilon_0 \cdot S)$, where ε_0 is the dielectric constant of vacuum, i.e. 8.85×10^{-12} F·m^{-1}, and d is the thickness of the gap between the electrodes and S is the contact area of the electrodes. The dielectric constant (ε) and dielectric loss tangent (tan δ) of the suspensions at 2 kHz frequency are listed in Table II.

A dielectric loss model has been proposed by Hao *et al.* [1]. In this model, they indicated that both ER and non-ER particles can be polarized under an electric field, and in this process the particle dielectric constant is dominant; however, after the particle polarization, the ER particles can re-orientate along the electric field direction, building fibrillated bridges between two electrodes, determined by the particle dielectric loss. The non-ER particles, however, are incapable of doing so. This is probably because the ER particles have a large dielectric loss tangent, which could generate a large amount of bound surface charge. Therefore, the dielectric loss of the particles plays a more important role than the dielectric constant, in influencing the ER effect of a material. A good ER material, thereby, should have a relatively large dielectric loss tangent.

The dielectric properties of samples 1–6 (see Table II) indicate that the dielectric loss tangent (tanδ = 0.092) and dielectric constant (ε=2.25) of the suspension of sample 6, which has the best ER performance, is the largest; whereas, those of sample 1 (dried cellulose) (0.015 and 1.36), which has the lowest ER activity, are the smallest among the ER fluids of these samples. Samples 3–6 [Cellulose(-P-O)$_3$RE], which have better ER performance, exhibit higher tanδ values than sample 2.

Comparing sample 2 to samples 3 and 4, the ER activity of sample 2 is lower, even though its dielectric constant ($\varepsilon = 1.67$) is larger. This can be attributed to its smaller dielectric loss tangent ($\tan\delta = 0.029$), which impairs its ability of turning along the electric field direction and building the fibrillated bridges between the two electrodes [1]. In the comparison of samples 3–6, we have noticed that the η_E value (9562 mPa·s) of sample 4 is the largest, but its η_r value is the smallest (23.4) due to a large η_0 value (409.5 mPa·s). Therefore, the ER activity of sample 4 is the lowest among the cellulose(-P-O)$_3$RE materials, which can also be attributed to its low $\tan\delta$ (0.038). The $\tan\delta$ value of sample 3 (0.063) is close to that of sample 5 (0.067). This makes the η_r value of sample 5 (24.3) only slightly lower than that of sample 3 (25.5), even though the ε value of sample 5 (1.90) is larger than that of sample 3 (1.46). Hence, the experimental results of the electrorheological and dielectric properties of these materials show that the dielectric loss tangent can play a dominant role in influencing ER effect of the material, and the correlation between the dielectric property and the ER effect is consistent with the empirical criterion obtained by Hao *et al*. [20].

The ER performance of the cellulose(-P-O)$_3$Y material is the best among all cellulose(-P-O)$_3$RE materials. This may be explained by the remarkable differences in their electron configurations, which can cause a difference in the polarizability of the yttrium and lanthanide complexes, since the Y^{3+} ion does not have any *f*-electrons. As for the relationship between the different rare earth ions and their ER activity, more work needs to be done in order to derive a detailed mechanism.

The dependencies of the shear stress and apparent viscosity of the suspension on shear rate under different electric field strengths for sample 6 [cellulose(-P-O)$_3$Y] are illustrated in Fig. 4. The shear stress increases linearly but very slowly [see Fig. 4a], and the apparent viscosity remains constant [see Fig. 4a], with increasing shear rate when no electric field is present. This shows that the suspension exhibits the behavior of a Newton fluid without an applied electric field. However, under an electric field, the dependency of shear stress on shear rate is related to the applied electric field strength at larger shear rate ($\dot{\gamma} > 50\,S^{-1}$). The shear stress increases slowly at $E > 2.2$ kV/mm, but decreases slowly at $E \leq 2.2$ kV/mm, with increasing shear rate [see Fig. 4a]. Therefore, it is obvious that the interfacial polarization between the dispersed phase and the medium in the suspension is affected strongly by the electric field strength. Under higher electric field strength, the electrostatic interaction force between the particles, which originated from the induced dipole moment caused by the interfacial polarization, dominates the shear force at $E > 2.2$ kV/mm; that is to say, the chain-like structure, which is established by the electrostatic interaction between the particles, is not fully broken even at high shear rates, but the electrostatic interaction force between the particles is weaker under low electric field strength than under high electric field strength. Consequently, at $E \leq 2.2$ kV/mm and $\dot{\gamma} > 50\,S^{-1}$, the shear force plays a dominant role, the destruction rate of the particle chain structure exceeds its reformation rate, and the chain-like structure would be broken gradually with increasing shear rate. The apparent viscosity of the suspension in an electric field augments drastically at first, thereafter falls, and the decline in viscosity reduces gradually, with increasing shear rate [see Fig. 4b]. Therefore, as a characteristic ER fluid, the suspension shows the behavior of a non-Newton fluid.

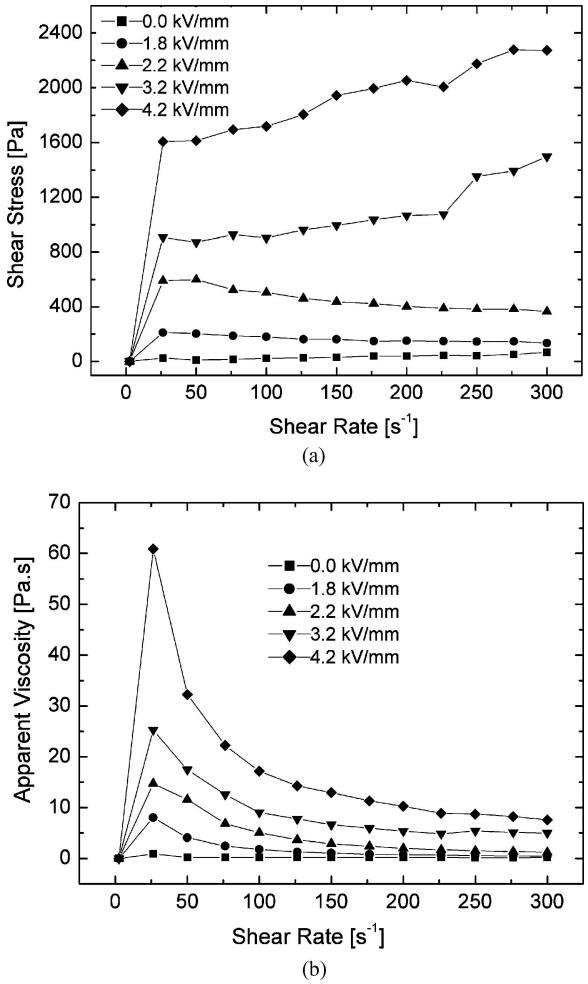

Figure 4 Dependence of shear stress (a) and apparent viscosity (b) of ER suspension on shear rate under various electric field for sample 6.

3.3. Surface area and ER effect of materials

The polarizability of these polymeric molecules should be a crucial factor in influencing the ER effect of the materials, because the polarizability is related to the dielectric loss tangent of a material, and the interfacial polarization between the dispersed phase and the medium in the suspension under an electric field. It is well known that the grain size, surface properties, and composition of the particles, which can influence the physical and chemical nature of a material, are essential to the dielectric and polarization properties of the material.

Hao *et al*. [21] have elucidated the physical ground of the ER effect, and the possible ER mechanism has been proposed as follows: a large interfacial polarization would facilitate the particle to attain a large amount of charges on the surface, then lead to the turn of the particle along the direction of an electric field to form a fibrillation structure; the strength of the fibrillation chains is thus determined by the particle polarization force, i.e., the particle dielectric constant. At the same time, they indicated that if the particle surface charge density is d, its surface area is S, and the particle is uniform, then one single particle bounds charge $q_s = Sd = k_1 E$, where E is the electric field strength, k_1 is a constant, $k_1 = S\varepsilon_s/4\pi$, and ε_s is the static dielectric constant. Using this equation, one can estimate the critical (minimum) electric field strength required to drive a particle to turn. The particle turning process is very important for the ER effect; therefore, the magnitude of the q_s value should be related to the ER effect. Based on these results we can see that the surface area of the particles would influence the ER effect of a particle material. In order to further investigate the impact of the particle surface area on the ER effect of the polymer materials, the surface area of the samples were measured. The results show that the cellulose(-P-O)$_3$RE particles (samples 3–6), which exhibit better ER activity, have larger surface areas (1.2–2.1 m^2/g) than that of the cellulose-P-ONH$_4$ particles (1.1 m^2/g) (sample 2). However, the ER activity of the cellulose particle material is the weakest (see Section 3.2), even though its surface area (1.8 m^2/g) is larger. This phenomenon can be ascribed to the fact that the polarizability of the cellulose particle material is the lowest among these materials. In other words, a material's polarizability seems to play a more important role than its surface area in determining the ER performance.

Comparing the grain sizes (see Fig. 1), we can see that the grain sizes of the cellulose(-P-O)$_3$RE particles are much smaller than that of the cellulose-P-ONH$_4$ particles. This shows that the average grain size of the polymeric particles may decrease with the formation of the rare earth complex, at the same time, the surface area of the material may increase, and this can be an important reason why the ER activities of the cellulose(-P-O)$_3$RE materials are stronger than that of the cellulose-P-ONH$_4$ material. Moreover, the rod-like and irregular particles shape for the cellulose-P-ONH$_4$ material, which may make the difficulty in the turn of the particle along the direction of an electric field to form a fibrillation structure, would influence its ER performance; so, this type of particle shapes may be a factor to induce its lower ER activity than the cellulose(-P-O)$_3$RE materials.

3.4. Thermal stability of materials and anti-sedimentation stability of suspension

The results from thermal analyses indicate that the decomposition temperature (323°C) of microcrystalline cellulose falls with the esterification reaction, but the decomposition temperatures (265–270°C) of cellulose(-P-O)$_3$RE are higher than that of cellulose-P-ONH$_4$ (247°C), which is in agreement with a known rule, namely the thermal stability of the ammonium salt is lower than that of the metal salt due to strong polarization ability of the proton in the ammonium salt when their corresponding anion is the same. Therefore, the rare earth complexes materials [cellulose(-P-O)$_3$RE] exhibit higher thermal stability than the cellulose-P-ONH$_4$ material. In practical applications, the ER material with higher decomposition temperature should be more beneficial.

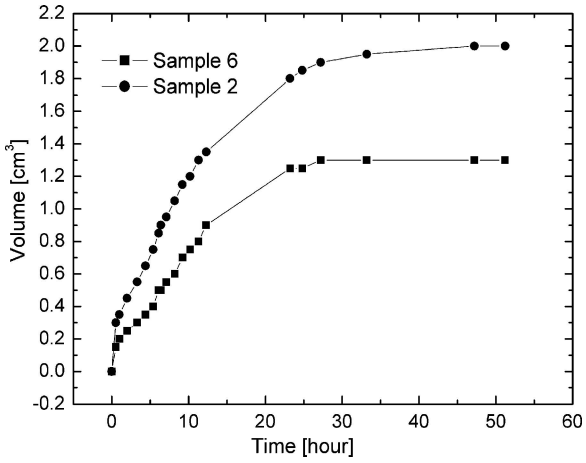

Figure 5 The flow curves of the volume change of pure silicone oil above the suspension containing the particles in the sedimentation process of the particles with time for sample 2 and 6.

The stability of the suspensions of the cellulose-P-ONH$_4$ and cellulose(-P-O)$_3$Y materials in dimethyl silicone oil has been measured with the following method: the material (1.00 g) is dispersed in dimethyl silicone oil (4.00 g) by mixing fully in a measuring cylinder with a 1.2 cm diameter. The volume of pure silicone oil above the suspension containing the particles in the sedimentation process of the particles is observed according to schedule. The volume change with time is displayed in Fig. 5. The results show that, the deposition of the cellulose-P-ONH$_4$ material is much faster than the cellulose(-P-O)$_3$Y material; moreover, after 27 h of the sedimentation process, the suspension remains in a stable state, no more volume change was detected in another 24 h, when the volume of the suspension is larger for sample 6 (3.6 cm^3) than for sample 2 (2.9 cm^3). Namely, the ER fluid containing the cellulose(-P-O)$_3$Y material is more stable than the ER fluid containing the cellulose-P-ONH$_4$ material. This shows that the density of the polymeric material may decrease when ammonium ions are replaced with RE ions to form RE complexes. This is probably because in the polymeric RE complex, each RE ion is coordinated by three -P-O groups, and this could increase the crimp degree of the polymer chains and decrease the interactions between them.

In addition, the effect of the rare earth content on ER property of the materials mentioned above are currently under investigation, the yttrium content (3.26 wt%) in

cellulose(-P-O)$_3$Y material is a optimum value; other investigation results will be reported.

4. Conclusions

A New class of ER material, cellulose(-P-O)$_3$RE (RE = Ce, Gd, Er and Y) complexes, has been synthesized by the reaction between cellulose-P-ONH$_4$ and RE(NO$_3$)$_3$ solutions. The ER performance, dielectric properties, and surface area of the cellulose, cellulose-P-ONH$_4$ and cellulose(-P-O)$_3$RE materials are studied. The results show that the ER activity of the cellulose material is the weakest, and the cellulose(-P-O)$_3$RE materials have better ER activity than the cellulose-P-ONH$_4$ material; furthermore, the cellulose(-P-O)$_3$Y material exhibits the best ER activity among these materials. The dielectric loss tangent (tan δ)can be a dominant factor in affecting the ER property of the materials, whereas the effect of the size, shape and surface area of the particles on their ER performance is not negligible either. In addition, the cellulose(-P-O)$_3$RE materials showed better thermal stability, and their suspensions are more stable in the anti-sedimentation than that of the cellulose-P-ONH$_4$ material.

Acknowledgements

This Project is supported by the State Key Laboratory of Vehicle Transmission (51457030103 JW0201), the National Natural Science Foundation of China (20023005, 29831010) and the National Key Project for Fundamental Research (G1998061305).

References

1. T. HAO, *Advances in Colloid and Interface Science* **97** (2002) 1.
2. H. BLOCK and J. P. KELLY, *J. Phys. D: Appl. Phys.* **21** (1988) 1661.
3. S. P. COUTER, K. D. WEISS and J. D. CARLSON, *J. Intell. Mater. Syst. Struct.* **4** (1993) 248.
4. T. HAO, *Adv. Mater.* **13** (2001) 1847.
5. X. P. ZHAO, C. R. LUO and Z. D. ZHANG, *Opt. Eng.* **37** (1998) 1589.
6. J. J. FAN, X. P. ZHAO, X. M. GAO and C. N. CAO, *J. Phys. D: Appl. Phys.* **35** (2002) 88.
7. X. P. ZHAO, Q. ZHAO and X. M. GAO, *J. Appl. Phys.* **93** (2003) 4309.
8. W. WEN, N. WANG, H. R. MA, Z. LIN, W. T. TAM, C. T. CHAN and P. SHENG, *Phys. Rev. Lett.* **82** (1999) 4248.
9. H. X. GUO, X. P. ZHAO, H. L. GUO and Q. ZHAO, *Langmuir* **19** (2003) 9799.
10. T. Y. GONG, D. T. WU and D. W. M. MARR, *Langmuir* **19** (2003) 5967.
11. D. G. BYTT, GB Patent, 2189803, 1987.
12. F. E. FILISKO and W. E. AMSTRONG, U.S. Patent, 4744914, 1988.
13. B. G. AHN, *Polymer Journal* **35**(1) (2003) 23.
14. D. P. PARK, J. Y. HWANG, H. J. CHOI, C. A. KIM and M. S. JHON, *Materials Research Innovations* **7**(3) (2003) 161.
15. B. G. AHN, U. S. CHOI, C. H. KIM and O. K. KWON, *Int. J. Mod. Phys. B* **15**(6–7) (2001) 1009.
16. S. G. KIM, J. W. KIM, W. H. JANG, H. J. CHOI and M. S. JHON, *Polymer* **42**(11) (2001) 5005.
17. U. S. CHOI and B. G. AHN, *Colloids and Surfaces A-Physicochemical and Engineering Aspects* **168**(1) (2000) 71.
18. K. NAKAMOTO, Infrared Spectra of Inorganic and Coordination Compound, 4th Ed., John Wiley & Sons Inc., New York, (1986).
19. K. NAKANISHI and P. H. SOLOMON, Infrared Absorption Spectroscopy, 2th Ed., Holden-Day Inc., San Francisco (1977).
20. T. HAO, Z. M. XU and Y. Z. XU, *J. Colloid Interface Sci.* **190**(2) (1997) 334.
21. T. HAO, A. KAWAI and F. IKAZAKI, *Langmuir* **14** (1998) 1256.

Received 11 April 2004
and accepted 17 May 2005